Short and long wire detection using high-frequency electromagnetic induction techniques

Benjamin Barrowes*[a], Danney R. Glaser,[a] Mikheil Prishvin,[b] Kevin O'Neill,[b] and Fridon Shubitidze[b]
[a]U.S. Army Engineer Res. and Dev. Center CRREL, 72 Lyme Rd., Hanover, NH, USA 03755
[b]Dartmouth College, 14 Engineering Drive, Hanover, NH, USA 03755

ABSTRACT

Thin wires are a critical component of many types of improvised explosive devices. Short wires with lengths on the order of 30 cm to a few meters are difficult to detect using electromagnetic induction metal detectors due to the induction currents having only a small cross-section of the wire to circulate on. Longer wires on the order of tens of meters up to a kilometer are often buried at depths which preclude induction detection. We demonstrate short wire detection and identification through acquiring the electromagnetic induction response at frequencies above the traditional EMI range. In addition, long wire detection and identification is shown through electric field coupling between excitation coils and the long wire itself. We present the relevant physics of detecting both types of wires and experimental and modeling results demonstrating the utility of this high-frequency EMI regime. We present a high-frequency electromagnetic induction instrument utilizing frequencies up to 15 MHz which can detect and classify both short and long wires.

Keywords: electromagnetic induction, improvised explosive devices, short and long wires, cables, wire bundles

1. INTRODUCTION

The US military has a need to detect non-metallic Improvised Explosive Devices (IEDs) and UneXploded Ordinance (UXO). The EMI sensors currently available for detection of metallic UXO and IEDs operate in the range of tens of Hertz to about 100 kiloHertz (kHz), with the time-domain sensors not exceeding an equivalent 10 kHz. Most metallic munition's polarization relaxation response is within the frequency range of the current low frequency EMI (LFEMI) geophysical sensors (below 100 kHz), and these sensors have proven effective for the detection and discrimination of said metallic munitions. Yet the anticipated EMI signatures from wires associated with non-metallic IEDs do not fall within the detection range of these systems. Some LFEMI techniques utilizing the ferrous or inductive response of metal infrastructure have long been used for subsurface utility detection including, pipes, cables, and utility wires such as power, telephone, and cable. Yet these systems tend to operate based on detection of long continuous conductors, often with an active input at one end, rather than the small wires necessary for detection of IEDs. Therefore, a new method for detecting smaller and/or less conducting targets is required. McKenna et al (2012) demonstrate the ability of an electromagnetic gradiometer for automated detection of tunnel related infrastructure, such as wires [1]. Recent advancements in high-frequency electromagnetic induction (HFEMI) techniques have demonstrated the ability to detect carbon rods, voids, and other non-metallic UXO and IED components [2],[3],[4]. This study examines the application of HFEMI to detection of the short and long wires associated with non-metallic UXO and IEDs, as well as command wires and tunnel infrastructure by exploiting frequencies above the standard LFEMI range [2].

Interrogation of the subsurface using electromagnetics is desirable for the fundamental reason that the ground does not have to be disturbed during interrogation. And recently with the advent of Unmanned Aerial Systems (UASs), the possibility of standoff interrogation during the which the ground is not touched or disturbed is now a reality. Ground Penetrating Radar (GPR), operating from perhaps 50 or 100 MHz to 950 MHz or more, has long been of interest for exploring the subsurface, whether for characterizing the medium and its configuration or for identifying inclusions. GPR systems operate by transmitting electromagnetic waves into the ground, and then recording reflections over time and space. Electromagnetic waves at these high frequencies will be partially reflected off of material boundaries representing contrasting dielectric conditions, while some of the energy will be transmitted through the contrasting material. While the

*Benjamin.E.Barrowes@usace.army.mil; phone (603) 646-4822

reflections typically do not contain information about the contrast boundary they reflected from, the change in propagation velocity can provide some material information, yet much of the information is essentially lost.

In contrast, electromagnetic induction (EMI) systems operate at much lower frequencies, typically 10s of Hz up to 50 or 100 kHz. At such low frequencies, the ground is mostly "transparent" because the skin depth is large given the conductivity of the soil. However, some drawbacks associated with EMI include the inability to guide EM waves and the rapid falloff of magnetoquasistatic fields with distance [5]. As such, all of the targets in this study are considered to be at close range, often within one or two antenna diameters of the sensor, though the long wire results could potentially be applied to targets at much greter separations. Glaser et al (2017), demonstrate the EMI response fall off associated with a single UXO at standoff increments of 0.10m [6],[7] applicable to transient topographical changes like snow events and erosion.

EMI sensors acquire information about the target being interrogated because of the penetration of currents into the target and the resulting eddy currents in the target which lead to a characteristic relaxation signature of the secondary magnetic field. EMI has performed well in recent land-based detection and discrimination tests for finding metallic targets such as UXO in the near subsurface (i.e. ~1 meter) [8-10]. However, Intermediate Electrically Conducting (IEC) subsurface targets, such as some IEDs and advanced weapons made from carbon fiber are not detectable with current low frequency EMI sensors [11-14] because less conducting materials exhibit a relaxation response to electromagnetic stimulation at frequencies greater than those used in the traditional EMI regime of up to 100 kHz (see Fig. 1).

Figure 1a demonstrates the generalized relationship between the in-phase and the quadrature of a theoretical conductive spherical target, while figure 1b shows this same expected response modeled for three spheres at three different conductivities. The HFEMI instrument occupies the shaded frequency range extensively expanding the detection range presently occupied by the standard and advanced LFEMI sensors.

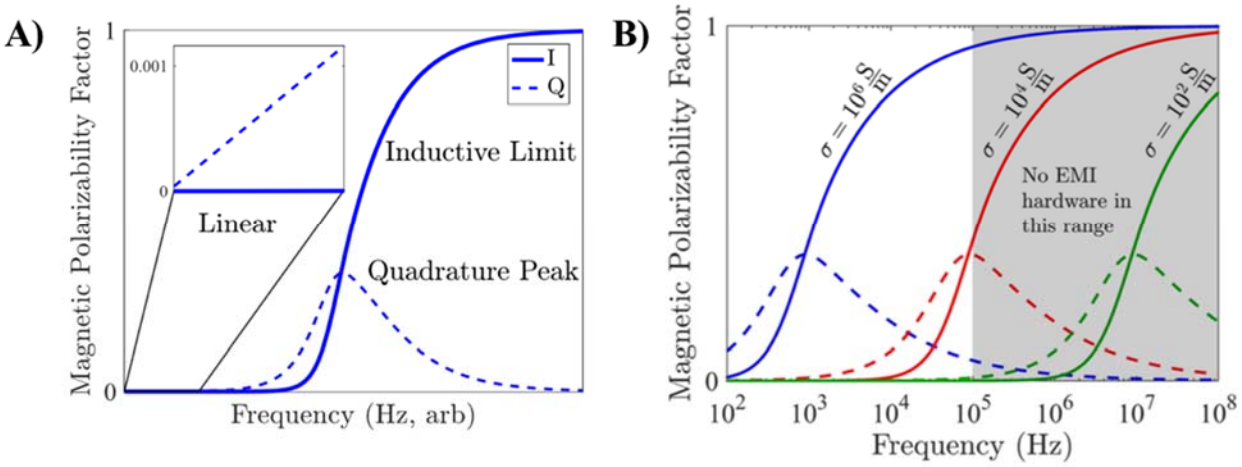

Figure 1 - A) Generalized EMI in-phase and quadrature components for a conducting, non-permeable sphere [2],[15]; and B) for three 8cm sphere (μ_r=0, ε_r=1) with varying conductivity [2].

2. HIGH-FREQUENCY ELECTROMAGNETIC INDUCTION METHODS

According to Lenz's law, a conducting object in a primary alternating magnetic field will develop eddy currents to oppose the changing flux inside the object [16]. These eddy current depend on the conductivity of the object. In metals, conductivity and electron mobility is high which allows induced opposing currents to form (again via Lenz's law) at lower frequencies than in lower conducting materials. In other words, the time rate of change of the inducing primary field needs to be higher (higher frequency) for materials with lower conductivity. In turn, these eddy currents produce a secondary alternating magnetic field, which is out of phase with the primary field. We call the component of the eddy current synchronized with the primary field (in-phase component) and 90° out-of-phase with the primary field (quadrature component) as shown in Figure 1 and in the figures below. Characteristics of these components of the secondary field are used as signatures of the target and to determine properties of the target such as size, shape, location, orientation,

permeability, and conductivity. In general, higher conductivities and larger targets result in lower peaks in the quadrature response [5].

In order to detect eddy currents in objects with lower conductivity than metals, the frequency range of traditional EMI sensors had to be increased. In order to sense the equivalent of 15 MHz in the time domain, a time domain instrument would need to turn off the primary magnetic field within fmax = $_{1\,Dt}$ (where $_{1\,Dt}$ is the transience of the primary field turnoff), or $_{1\,Dt}$ = 67ns, which is currently not feasible [17]. Therefore, we developed a frequency domain instrument that could operate at frequencies up to 15 MHz. A more thorough discussion of the iterations of our HFEMI instrument can be found in [18]. To summarize, we found that we needed to shorten the transmitter and receiver coils in order to avoid wave effects on the coils and the resulting field asymmetry. We have fabricated a hybrid coil system [19] to increase the signal-to-noise ratio at low frequencies.

Figure 2 provides a representation of the interrelationship of the transmitted field acting on a subsurface target and the measurement of the induced secondary field at the receiver coil. The transmit coil propagates an alternating magnetic field, which induces volume and surface currents in the target. The induced currents produce a secondary alternating electromagnetic field. The equations governing electromagnetic induction for the surroundings of the target are:

$$\nabla^2\Psi = 0 \tag{3}$$

where Ψ is the scaler potential of the magnetic field (B).

The magnetic field within the target is governed by

$$\nabla^2\overline{\Pi}_2 + k^2\nabla^2\overline{\Pi}_2 = 0 \tag{4}$$

where $\overline{\Pi}_2$ is the secondary magnetic field (A • m^{-1}) and k is the wave number of the target's material (m^{-1}).

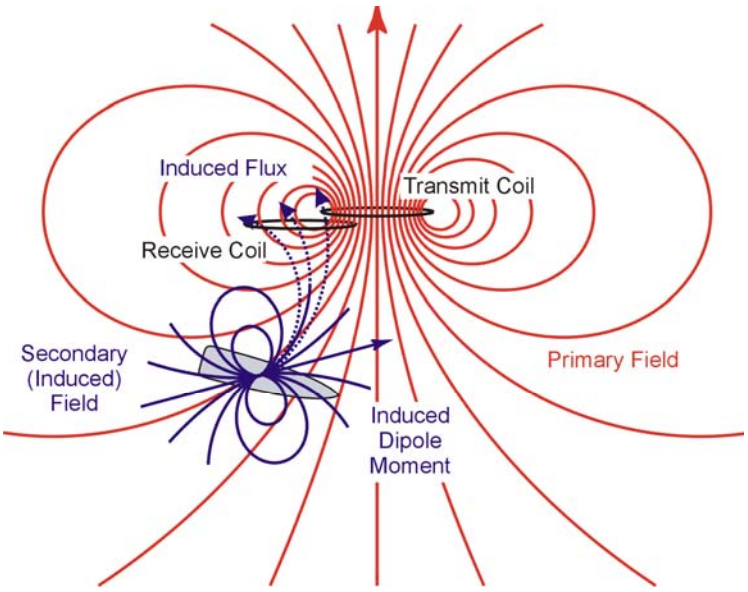

Figure 2 - Schematic of a typical electromagnetic induction system. Current in the transmit coil creates an alternating magnetic primary field. This field induces an alternating dipole moment in the target, which leads to a secondary magnetic field. This induced secondary field is detected by the receive coil, by which the target can be located.

The frequency at which the quadrature component of the secondary field is maximum is determined by the size, shape, permeability, and conductivity of the target. In general, the frequency of the relaxation peak is reduced by increased target size and reduced by increasing conductivity. EMI systems work well for detecting buried metallic targets because these typically have conductivities of $\approx 10^7 S \cdot m^{-1}$. Since wires have such a thin cross section, the relaxation peak is expected to occur at a much higher frequency than that for large UXO. The gauge of the wire should impact the induced response

with a thicker wire leading to lower relaxation peaks, but the length should not impact the induced response significantly because only a localized portion of the wire is exposed to the primary field.

At high enough frequencies, electric fields begin to play a role in the currents on a target such as a wire. High frequency currents in the primary coil can cause charges to move along the wire in addition to inducing charges to move in circles in the wire cross section. We refer to these currents along the wire at high frequencies as linear currents to distinguish them from induced currents. These linear currents radiate and will lead to a magnetic field due to the right hand rule, but this magnetic field is separate from the magnetic field caused by the induced currents.

Figure 3 demonstrates theoretical representations of the anticipated induction and radiation field patterns for targets consisting of short wires (figure 3a), long wires (figure 3b), and short cables (figure 3c). Note that induced currents in short wires are expected to oppose the change in the magnetic field, whereas linear currents on long wires are expected to align with the transmitted electric field. Short wire bundles or cables are expected to behave similarly to the individual short wires exhibiting an aggregate induced response.

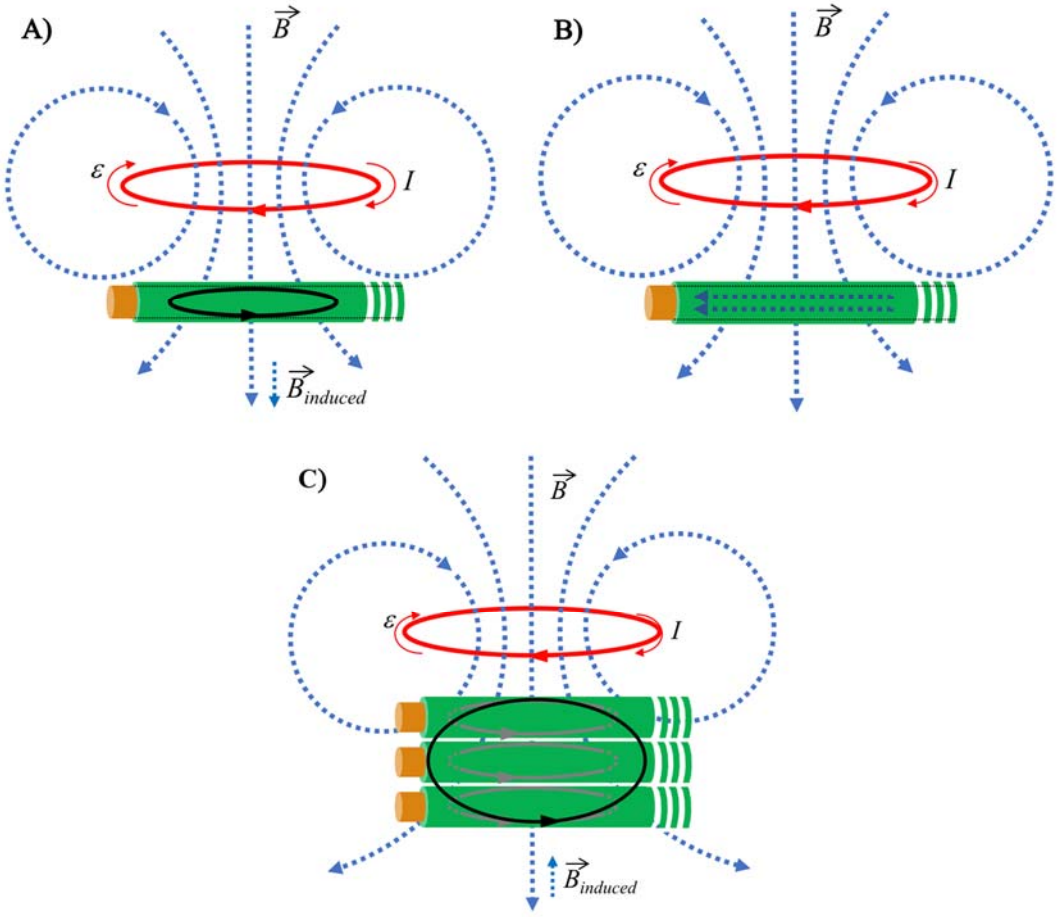

Figure 3 - Theoretical examples of the electromagnetic fields for short, long, and bundled wires: A) Short wire phenomena induced field; B) Long wire phenomena linear currents; C) short bundle wires phenomena induced field.

3. SHORT WIRE, SHORT CABLES, AND LONG WIRE DETECTION RESULTS & DISCUSSION

As indicated above, the expected response for short wires and short cables is similar based on an induction of electric current and the resulting magnetic field, while the magnetic field response for long wires is the result of a linear current along the wire, not an inductive circulating current. In this section, we compare the responses of wires with differing gauge, short wires with varying lengths, and results from measuring at different positions along the wire.

Figure 4a shows both the modeled and measured in-phase and quadrature responses of a 30 cm long 12 American wire gauge (AWG) wire over the frequency range from 10kHz to 15MHz. The model fits the measured inphase and quadrature responses well between 10kHz and 10MHz. Because we used fewer turns in our Tx and Rx coils, data at low frequencies are noisier than with traditional EMI sensors. In general it is clear the center frequency of the relaxation peak in the quadrature component of this data from this particular wire fragment is approximately 1.8MHz. Figure 4b shows the experimental set-up for the measurement. Note the overlapping receiver and transmitter coils. This configuration was chosen as an alternative to the figure 8 Rx coil method to maximize the response of the wire. In this case, the wire should be close to the edge of the Tx coil so that the electric field from the Tx coil will be the strongest and aligned with the wire under test.

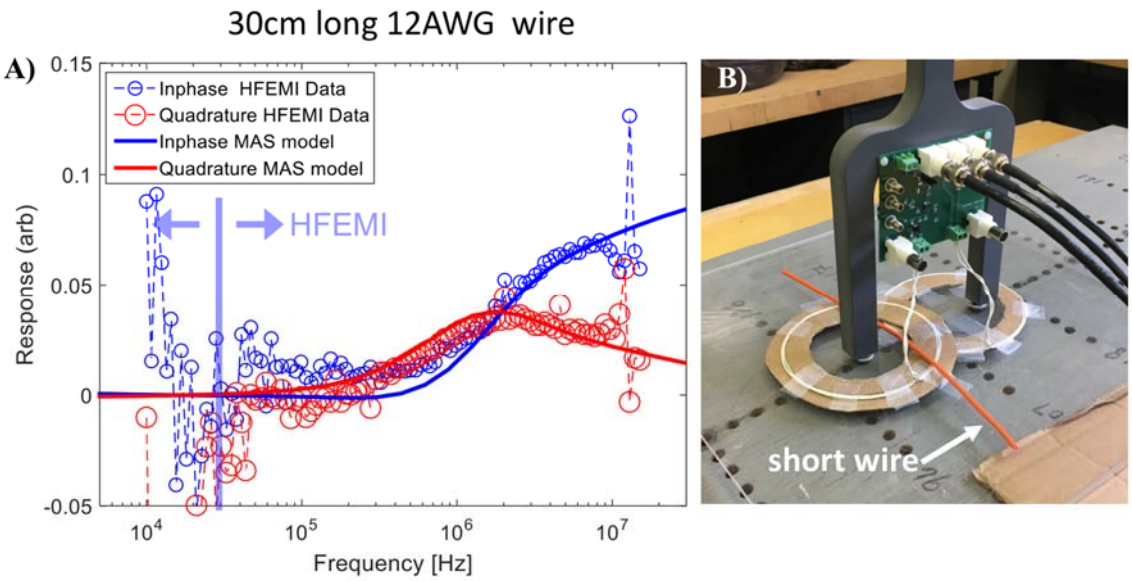

Figure 4 - A) HFEMI measurements (circles) and models (solid) for in-phase (blue) and quadrature (red) response of a 30-centimeter, 12-gauge wire; B) experimental set-up for the measurement displaying the HFMI antenna configuration.

The response for long wires as might be associated with tunnels or command wires is different when compared to the case of the short wires. The response as indicated in section 2 above, follows a pattern indicative of a linear current radiating rather than an induced current. We tested a 26 long wire to see whether we could cause a linear current along the wire. A 26 meter wavelength in free space corresponds to a frequency of about 3e8/26=11.5MHz. Due to end effects and coupling of the wire with the concrete and rebar in the floor, the full wavelength instead fits on this 26 meter wire at 7.5MHz with the half wave resonance occurring at 3.8MHz. These resonances suggest that indeed, linear currents are causing a radiated electromagnetic field around the wire in addition to an EMI magnetic field.

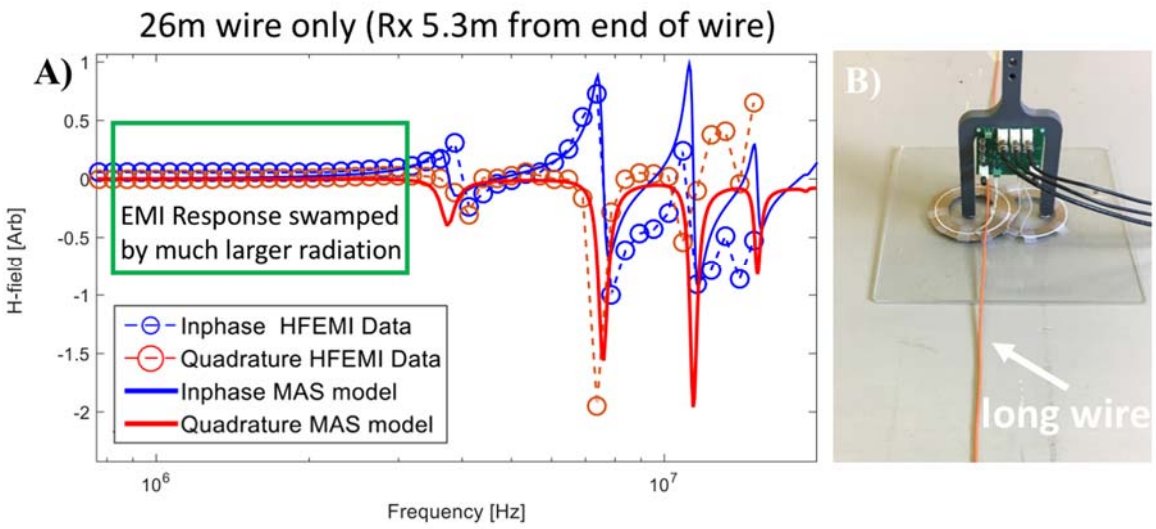

Figure 5 - A) HFEMI measurements (circles) and models (solid) for in-phase (blue) and quadrature (red) response and model of a 26-meter, 12-gauge wire, with the receiver positioned 5.3m from the end of the wire; B) experimental set-up for the measurement displaying the HFMI antenna configuration

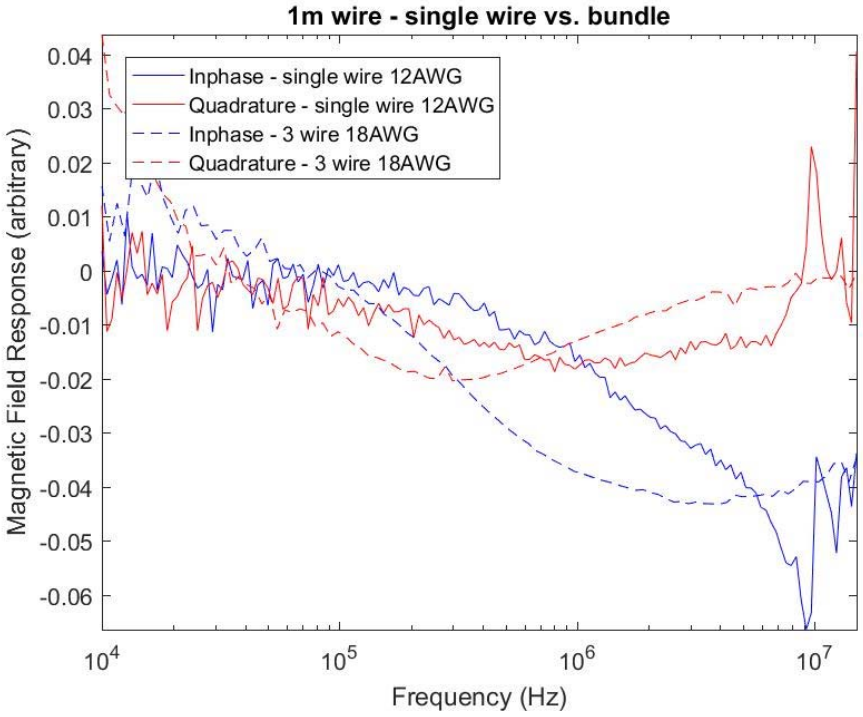

Figure 6. Short wire in-phase (blue) and quadrature (red) responses for a 1-meter length of 12AWG wire (solid) and a 1-m length of three 18AWG bundled wires (dashed). Note magnitude of the responses have been scaled for clarity.

Bundled wire responses were expected to behave as an aggregate target since the magnetic fields are in close proximity and interact as illustrated in Figure 3C. Figure 6 shows a comparison of in-phase and quadrature responses for a single 1 meter-long 12AWG wire compared with a bundle of 3, 18AWG wires 1 meter in length. Overall, they are of relatively the same magnitude and shape, however some obvious differences in response can be observed. First, the results of the three wire bundles appear to be more stable, with less noise than that of the single wire response. But the quadrature peak in the bundled wire response occurs at a lower frequency due to the interaction of the three wires, 300kHz as opposed to more than 1MHz for the single wire case.

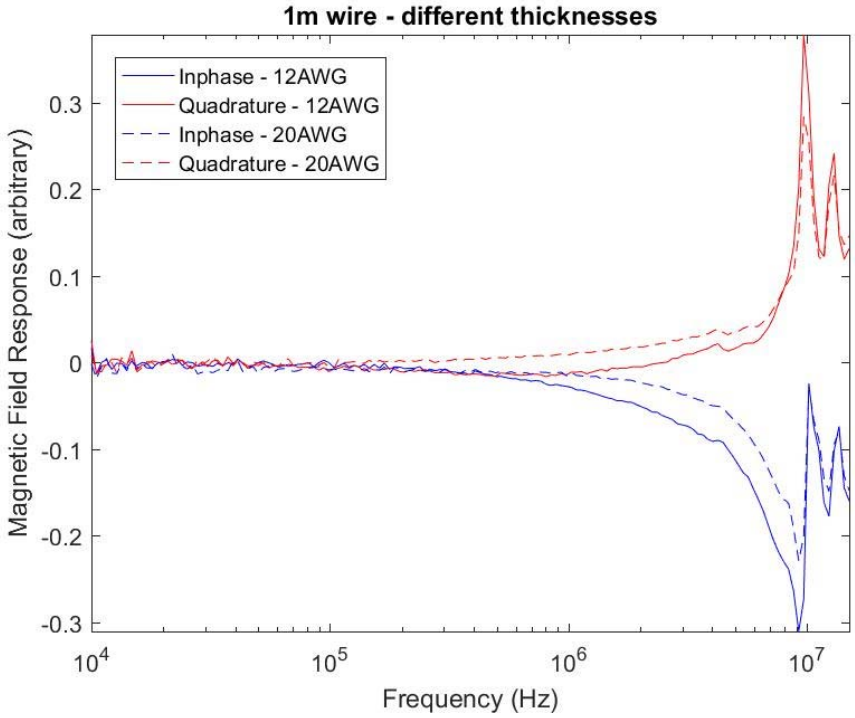

Figure 7. Short wire in-phase (blue) and quadrature (red) comparison for a 1-meter length of 12AWG wire (solid) and 20AWG wire (dashed). The relative responses are distinguishable in the 10^6 Hz to 10^7 Hz range.

We also evaluated the response of two single core wires one 12AWG and one 20AWG, each 1 meter in length. Figure 7 demonstrates the comparison of the in-phase and quadrature of these two targets. The responses are similar except that the induction response is much stronger for the 12AWG wire than for the 20AWG wire due to the increased thickness. At the highest frequencies the responses are similar (though noisy) demonstrating that the thickness of the wire does not have a significant effect on the linear current response.

Next, we considered the effects of length variations in the short wire targets. Examples of 0.3, 1.0, and 2.0 meters in length, 12 gauge wires were examined. The shorter the wire, the higher the frequency needed to excite linear currents on the wire. This can be seen in the inphase and quadrature responses in Figure 8 as longer wires have a larger response at lower frequencies. This information will be useful when designing target surveys and determining the frequency range necessary for a given wire length.

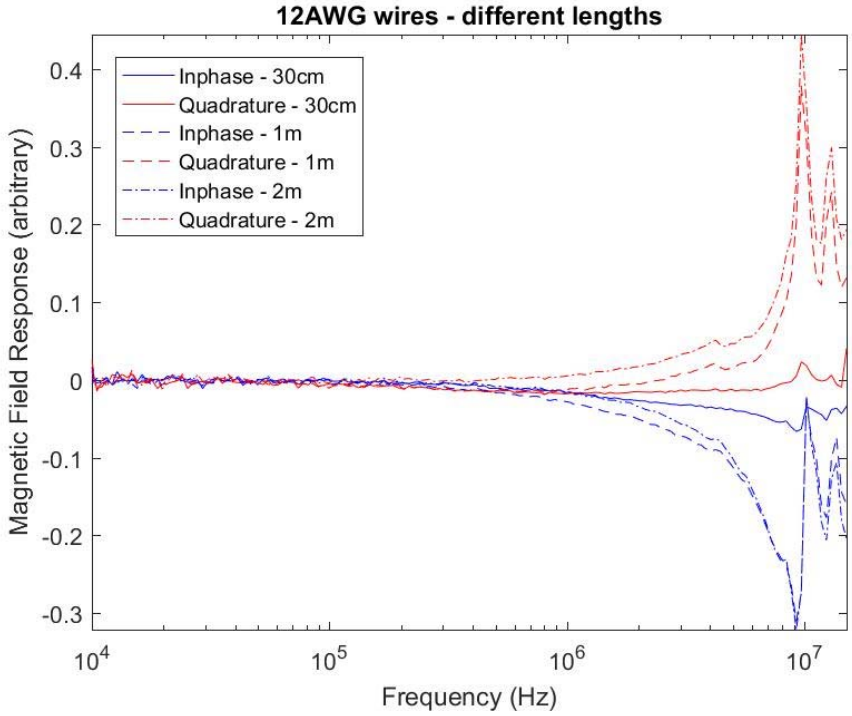

Figure 8. Short wire in-phase (blue) and quadrature (red) comparison for three lengths: 0.3 meters (solid); 1.0 meter (dashed); and 2.0 meters (dash-dot-dash). Note the tendency towards linear radiation response at lower frequencies as the length increases.

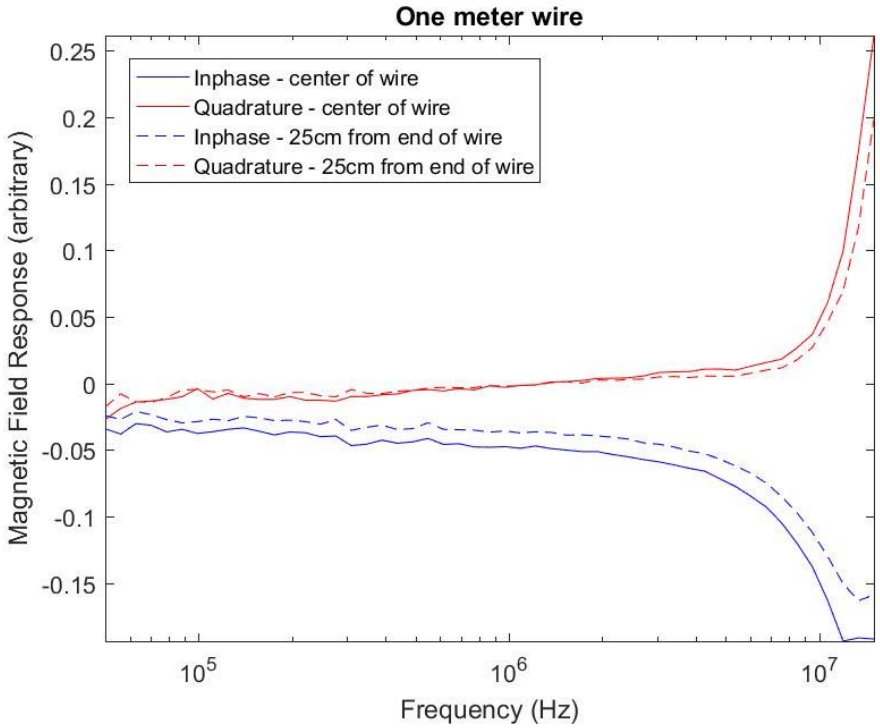

Figure 9. In-phase (blue) and quadrature (red) responses for a one-meter length of 12AWG wire measured at the center of the wire (solid) and at 0.25m from the end of the wire (dashed).

The last consideration for this study is regarding the sensor position relative to the ends of the wire targets. Figure 9 displays a comparison between measurements made at the center of a 1 meter long 12AWGwire, and the same measurements made 0.25 meters from one end. The location along the wire where the 0.25 meter measurement was made was of a lower amplitude in both the in-phase and quadrature responses for nearly all frequencies. This suggest the possibility of determining relative position along a length of wire from measurements if the proper inversion scheme is employed.

These observations could be very useful by non-invasively determining directionality which may be implemented when investigating the source or purpose of a buried wire. Rather than simply identifying the presence or a wire, by determining position along a wire, one might be able to determine relative direction towards the controls or IED, or in which direction a tunnel may lead.

4. CONCLUSIONS

Unique electromagnetic signatures associated with short wires, short wire bundles, and long command wires were observed using the US Army's high-frequency electromagnetic induction (HFEMI) sensor. Detection of these types of wires enhances the HFEMI systems ability to detect non-metallic IEDs as well as infrastructure associated with insurgent tunnels. This provides a direct benefit to the war-fighter and fills a gap in the currently available technology used to detect, characterize, and mitigate these threats. Using this sensor, the possibility now exists to determine the location of the wire, its orientation, and its length.

Future work will improve the range of detection of the HFEMI instrument. We also plan to develop inversion algorithms to better resolve the subsurface targets in specific soils. Improvements in data acquisition speed will facilitate large scale mobilization efforts. By separating the transmitting and receiving coils, we hope to evaluate the functionality of a multi-channel bi-static system that can interrogate volumes of earth, while improving data acquisition geometry. We will continue to optimize the construction materials to improve man-portability. Finally, we hope to deploy the system on a drone-based platform to reduce human exposure to harmful and potentially deadly IED detection and characterization activities.

ACKNOWLEDGMENTS

This research was sponsored by the US Army ERDC Environmental Quality and Installations UXO program and by the Office of Naval Research. Any opinions expressed in this paper are those of the authors, and are not to be construed as official positions of the funding agency or the Department of the Army unless so designated by other authorized documents.

REFERENCES

[1] S.P. McKenna, K.B. Parkman, L.J. Perren, and J.R. McKenna. Automatic detection of a subsurface wire using an electromagnetic gradiometer. IEEE Transactions on Geoscience and Remote Sensing, IEEE Transactions on Geoscience and Remote Sensing, 51(1): 132-139, 2013.

[2] J.B. Sigman, B.E. Barrowes, K. O'Neill, Y. Wang, J.E. Simms, H.H. Bennett Jr., D.E. Yule, and Fridon Shubitidze. High-Frequency electromagnetic induction sensing of non-metallic materials. IEEE Transactions on Geoscience and Remote Sensing, IEEE Transactions on Geoscience and Remote Sensing, 55(9): 5254-5263.

[3] B.E. Barrowes, F. Shubitidze, J. Sigman, J. Bennett, J.Simms, D. Yule, and K. O'Neill. Void and Landmine Detection Using the HFEMI Sensor. Proceedings of SPIE – The International Society for Optical Engineering 10182, pp. Detection of Sensing of Mines, Explosive Objects, and Obscured Targets XXII, 1018210 (3 May 2017); doi: 10.1117/12.2262619; https://doi.org/10.1117/12.2262619

[4] B.E. Barrowes, J. Sigman, Y. Wang, K. O'Neill, F. Shubitidze, J. Simms, J. Bennett, and D.E. Yule. Carbon Fiber and Void Detection Using High-Frequency Electromagnetic Induction Techniques. Proceedings of SPIE – The

International Society for Optical Engineering 9823, pp. Detection of Sensing of Mines, Explosive Objects, and Obscured Targets XXI, 1018210 (3 May 2016); doi: 10.1117/12.2224584; https://doi.org/10.1117/12.2224584
[5] Discrimination of Subsurface Unexploded Ordnance, SPIE Press, Bellingham WA, 2016.
[6] B. E. Barrowes, J. P. Fernandez, K. O'Neill, I. Shamatava, and F. Shubitidze, "Electromagnetic induction tools for discrimination of unexploded ordnance: From basic physics to blind tests," FastTIMES 20 , March 2015.
[7] "Classification applied to munitions response," 2016.
[8] D.R. Glaser, and A.M. Wagner. Dynamic cold regions terrain effects on time-domain electromagnetic induction data. Cold Regions Science and Technology, (*In Review*).
[9] D.R. Glaser, A.M. Wagner, A.B. Gelvin, S. Saari, A. Staples, and G. Larsen, Snow Depth Calibrations for Electromagnetic Induction Investigations at a Former Munitions Waste Disposal Site in Alaska. American Geophysical Union Fall Meeting, Dec 2017.
[10] F. Shubitidze, B. Barrowes, J. Sigman, Y. Wang, I. Shamatava, and K. O'Neill, "Detecting and classifying small and deep targets using improved emi hardware and data processing approach," Proceedings of SPIE - The International Society for Optical Engineering 9072 , pp. The Society of Photo–Optical Instrumentation Engineers (SPIE) –, (Baltimore, MD, United states), 2014.
[11] 5. S. A. Grant, B. E. Barrowes, F. Shubitidze, and S. A. Arcone, "Homemade explosives in the subsurface as intermediate electrical conductivity materials: A new physical principle for their detection," Proceedings of SPIE – The International Society for Optical Engineering 9072 , pp. The Society of Photo–Optical Instrumentation Engineers (SPIE) –, (Baltimore, MD, United states), 2014.
[12] F. Shubitidze, J. Sigman, K. O'Neill, I. Shamatava, and B. Barrowes, "High frequency electromagnetic induction sensing for non-metallic ordnances detection," Proceedings of International Seminar/Workshop on Direct and Inverse Problems of Electromagnetic and Acoustic Wave Theory, DIPED , pp. 180 – 182, (Tbilisi, Georgia), 2014.
[13] F. Shubitidze, B. Barrowes, J. B. Sigman, J. Simms, J. Bennett, D. Yule, I. Shamatava, , and K. O'Neill, "Detection and discrimination subsurface low conducting buried hazards in a cluttered environment," SEG Symposium on the Application of Geophysics to Engineering and Environmental Problems , 2016.
[14] F. Shubitidze, B. E. Barrowes, J. B. Sigman, K. O'Neill, and I. Shamatava, "Uxo classification procedures applied to advanced emi sensors and models," Proceedings of International Seminar/Workshop on Direct and Inverse Problems of Electromagnetic and Acoustic Wave Theory, DIPED 2016-December , pp. 173 – 177, (Tbilisi, Georgia), 2016.
[15] J. R. Wait, "A conducting sphere in a time varying magnetic field," Geophysics 16 , pp. 666–672, 1951.
[16] Field and Wave Electromagnetics, vol. 2, Addison-Wesley, New York, 1989.
[17] C. Nelson, C. Cooperman, W. Schneider, D. Wenstrand, and D. Smith, "Wide bandwidth time-domain electromagnetic sensor for metal target classification," IEEE Transactions on Geoscience and Remote Sensing 39 (6), pp. 1129– 1138, 2001.
[18] J. E. Simms, J. B. Sigman, B. E. Barrowes, H. H. B. Jr., D. E. Yule, K. O'Neill, and F. Shubitidze, "Initial development of a high-frequency emi sensor for detection of subsurface intermediate electrically conductive (IEC) targets," Journal of Environmental & Engineering Geophysics - Near Surface Geophysical Letters , accepted for publication 2017.
[19] J. B. Sigman, B. E. Barrowes, Y. Wang, H. J. Bennett, J. E. Simms, D. E. Yule, K. O'Neill, and F. Shubitidze, "Coil design considerations for a high-frequency electromagnetic induction sensing instrument," Proceedings of SPIE – The International Society for Optical Engineering , 2017.